

## Plasma fluctuations and x-ray laser transverse coherence

Peter Amendt\*

*Lawrence Livermore National Laboratory, University of California, Livermore, California 94550*

Moshe Strauss†

*Nuclear Research Centre, Negev, Israel*

Richard A. London‡

*Lawrence Livermore National Laboratory, University of California, Livermore, California 94550*

(Received 3 May 1995)

The effect of plasma fluctuations on transverse spatial coherence of x-ray lasers is investigated. Hose type (random) transverse displacements of the x-ray lasing medium induced by pump-laser nonuniformities are considered in detail. Such displacements lead to decreased transverse coherence via reduced gain discrimination from mode coupling. This effect may be related to a previously reported insensitivity of transverse coherence to laser length in neonlike selenium at 206 and 210 Å [Trebes *et al.*, Phys. Rev. Lett. **68**, 588 (1992)].

PACS number(s): 42.50.Ar, 42.55.Vc, 42.60.Da, 52.25.Nr

Improving the transverse spatial coherence of x-ray lasers remains an essential goal in realizing their utility for biological imaging or x-ray holography [1]. Previous experimental studies of a selenium x-ray laser at 206 and 210 Å have shown that the time-integrated spatial coherence perpendicular to the foil is equivalent to that of a quasimonochromatic spatially incoherent disk source with diameter ranging from 100 to 600  $\mu\text{m}$  [2]. The associated transverse coherence length at the output of the laser spans only 0.2–1.3  $\mu\text{m}$ , which is an order of magnitude smaller than required for practical holographic studies. Efforts are underway to improve coherence and x-ray fluence by using multipass architectures [3] along with curved targets for reducing x-ray losses due to refractive defocusing [4].

Methods used to understand spatial coherence include modal analyses [5–7], numerical solutions of the paraxial wave equation [8], ray optics estimates [9,10], and Wentzel-Kramers-Brillouin (WKB) approximations [11–13], all of which predict generally increasing coherence with laser length. However, in Trebes *et al.* [2] the observed coherence length was lower by a factor of 5 compared to theory and failed to improve as the length of the laser increased. Proposed causes for the lower-than-expected coherence are time-averaged source motion [2] and measured off-axis peak radiation intensity profiles where coherence is argued to be lower [12]. However, these explanations fail to predict a lack of coherence improvement when the laser length is increased.

In this paper we generalize the modal approach to include fluctuation-induced mode coupling for exploring the interplay between laser-induced (random) source motion and gain length saturation as a possible explanation for the observed limitation on transverse coherence in Nova x-ray laser experiments.

We concentrate on one particular class of fluctuation that may be present in Nova two-beam x-ray laser experiments. A thin ( $\approx 750\text{-\AA}$ ) CH-backed target foil is irradiated on both sides by separate uncorrelated pump laser beams, each with a nearly 10–15% speckle intensity variation [14]. These intensity variations are correlated over distances along the line focus on the order of a speckle width (or diffraction-limited spot size)  $l_s = 2f\lambda$  and persist over the duration of x-ray lasing ( $\approx 200$  psec). The line-focusing architecture employs  $f/4.3$  ( $\approx f/4.4$ ) optics across (along) the line focus, giving  $l_s$  on the order of 10  $\mu\text{m}$ . The random intensity fluctuations, in turn, can imprint at early-time small transverse (horizontal) displacements  $x_0(z)$  of the x-ray lasing medium from the target symmetry axis, where  $z$  is along the line focus. These displacements are associated with “hose-type” fluctuations, as shown in Fig. 1. We can estimate the magnitude of  $x_0(z)$  using a simple inverse bremsstrahlung absorption model valid at early times before the plasma density becomes subcritical. If an imposed intensity imbalance on the two sides of the foil is given by  $\Delta I$ , then a net pressure imbalance locally arises across the foil (distributed over a speckle width) and is given by  $\Delta P \approx \nu \tau_s \Delta I / c$ . Here,  $\nu = \nu_{ei} \omega_{pe}^2 / \omega^2$  is the inverse bremsstrahlung absorption rate,  $\nu_{ei}$  is the

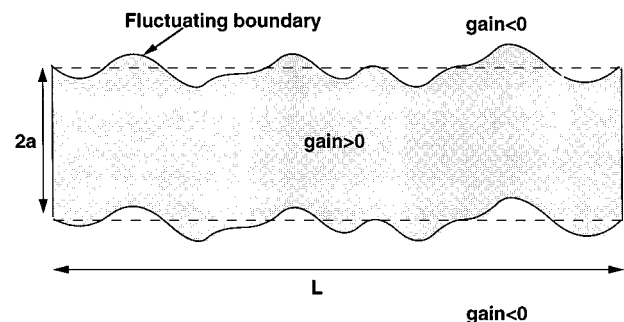


FIG. 1. Diagram of hose-type fluctuations of lasing (positive gain) medium induced by laser nonuniformities.

\*Electronic address: amendt1@llnl.gov

†Electronic address: moshe@black.bgu.ac.il

‡Electronic address: rlondon@llnl.gov

electron-ion collision rate,  $\omega_{pe}$  is the plasma frequency,  $\omega = 2\pi c/\lambda$ , and  $\tau_s$  is the duration of the intensity imbalance. Using momentum balance, we find  $x_0/l_s \approx (\nu\tau_s)(\Delta I/I)(I\tau_s^2/c\rho a l_s)/2$ , where  $a$  is the foil half-width, and  $\rho$  is the lasant mass density. For a Ne-like Se x-ray lasing plasma with  $\rho a \approx 4 \times 10^{-5}$  g/cm<sup>2</sup>,  $\Delta I/I \approx 0.15$ ,  $\tau_s \approx 200$  ps,  $\nu \approx 5 \times 10^{11}$  sec<sup>-1</sup> ( $T_e \approx 1.5$  keV),  $I \approx 7 \times 10^{13}$  W/cm<sup>2</sup>, we obtain  $x_0/l_s$  on the order of 0.1. This estimate is in satisfactory agreement with LASNEX hydrodynamic simulations [15].

An important dimensionless parameter characterizing the effect of such hose-type random fluctuations of the lasing medium on transverse coherence is obtained below in Eq. (10) from a modal analysis [5–7] of the laser electric field:  $\sigma_f = 4l_s \langle (dx_0/dz)^2 \rangle / g_0 a^2$ , where  $g_0$  is the x-ray laser gain strength, angular brackets denote ensemble averaging, and  $dx_0/dz = \pm \sqrt{\langle x_0^2 \rangle} / l_s$  is an assumed random telegraph signal (RTS) bivalent variable [16]. Using  $g_0 \approx 4$  cm<sup>-1</sup> and  $a \approx 100$   $\mu$ m (at 400 psec) we find  $\sigma_f$  to be on the order of 0.1. As we now show, this level of fluctuations in Nova two-beam x-ray lasing plasmas is sufficiently large to greatly reduce transverse coherence.

We now analyze in detail the role of hose-type fluctuations on degrading transverse coherence in x-ray lasers. Our starting point is the modal analysis of previous work [5–7] generalized to include variations in the  $z$  direction through the (normalized) hose-type transverse variable:  $\tilde{x} = [x - x_0(z)]/a$ . The field equation in the paraxial approximation, after neglecting the spontaneous noise source term, reads

$$\left[ \frac{\partial^2}{\partial \tilde{x}^2} - 2i \frac{\partial}{\partial z} - F_e(\eta \hat{h}(\tilde{x}) - i \hat{g}(\tilde{x})) \right] E(\tilde{x}, z) = 0, \quad (1)$$

where  $F_e = k g_0 a^2$  is the ( $z$ -independent) effective Fresnel number,  $k$  is the free-space longitudinal wave number of the electric field  $E$ ,  $\eta = h_0/g_0$  measures the refraction strength,  $\hat{h}$  is the normalized transverse electron density profile,  $\hat{g}$  is the normalized transverse atomic gain profile, and  $z$  is normalized to  $ka^2$ . We next expand the laser electric field  $E(\tilde{x}, z) = \sum_n c_n(z) u_n(\tilde{x})$  and define the density matrix  $\rho_{nn'}(z) \equiv c_n c_{n'}^*$ , where  $u_n(\tilde{x})$  satisfies the transverse eigenmode equation

$$\left[ \frac{d^2}{d\tilde{x}^2} - F_e(\eta \hat{h}_s(\tilde{x}) - i \hat{g}_s(\tilde{x})) \right] u_n(\tilde{x}) = -E_n u_n(\tilde{x}), \quad (2)$$

written in terms of square profiles, i.e.,  $\hat{h}_s, \hat{g}_s = 1$  for  $|\tilde{x}| \leq 1$  and zero otherwise. The appropriate *positive* gain eigenmodes are

$$u_n(\tilde{x}) = N_n \begin{cases} \cos(\alpha_n \tilde{x}) & (\text{even parity}) & |\tilde{x}| \leq 1 \\ \sin(\alpha_n \tilde{x}) & (\text{odd parity}) & |\tilde{x}| \leq 1 \\ A_n e^{\pm i \beta_n \tilde{x}} & & |\tilde{x}| > 1 \end{cases} \quad (3)$$

where the  $+$  ( $-$ ) sign is for  $\tilde{x} > 1$  ( $\tilde{x} \leq -1$ ),  $N_n = (1 + i/\beta_n)^{-1/2}$ ,  $\alpha_n^2 = \beta_n^2 - F_e(\eta - i)$ ,  $n = \{0, 1, \dots, n_{\max}\}$ , and  $A_n$  is obtained from the continuity condition at  $\tilde{x} = \pm 1$ . Using the fact that the eigenfunctions of the square profile generate a complete set [17], we expand  $E(\tilde{x}, z)$  in Eq. (1)

for a general potential in terms of square profile eigenmodes, giving with the use of Eq. (2),

$$\sum_n \left[ -2i \frac{\partial}{\partial z} - F_e(\eta \Delta \hat{h} - i \Delta \hat{g}) - E_n \right] c_n(z) u_n(\tilde{x}) = 0, \quad (4)$$

where  $\Delta \hat{h} = \hat{h} - \hat{h}_s$ ,  $\Delta \hat{g} = \hat{g} - \hat{g}_s$ , and the eigenvalue  $E_n = \beta_n^2$  is independent of  $\tilde{x}$ . Next, we multiply Eq. (4) by  $u_m(\tilde{x})$  and use the biorthonormal condition,  $\int u_n(\tilde{x}) u_m(\tilde{x}) d\tilde{x} = \delta_{mn}$ , to give

$$\frac{d}{dz} c_m + \sum_n (-\Lambda_{mn} + K_{mn}) c_n = 0, \quad (5)$$

where  $\Lambda_{mn} = i E_n \delta_{mn}/2 + D_{mn} = \Lambda_{nm}$ ,  $D_{mn} = F_e/2 \int (i \eta \Delta \hat{h} + \Delta \hat{g}) u_m(\tilde{x}) u_n(\tilde{x}) d\tilde{x}$  describes departures from square density and gain profiles, and  $k_{mn} = \int u_m(\tilde{x}) [\partial u_n(\tilde{x}) / \partial z] d\tilde{x}$  describes the coupling between the  $m$ th and  $n$ th modes due to fluctuations. In matrix form, Eq. (5) becomes  $dC/dz + (-\Lambda + K)C = 0$ . To solve for the matrix  $C$ , we diagonalize  $\Lambda$  using the eigenvalue equation,  $\Lambda v_l = \lambda_l v_l$ , where  $v_l$  is an eigenvector,  $\lambda_l$  is the corresponding eigenvalue, and  $v_l$  satisfies the orthonormality condition:  $v_l v_{l'} = \delta_{ll'}$ . Defining a matrix  $R$  with  $\{v_l\}$  as columns and a diagonal matrix  $\lambda$  with eigenvalues  $\{\lambda_l\}$  along the diagonal, we have  $\Lambda R = R \lambda$ . Defining the *reduced* state vector  $C^{(1)} \equiv R^T C$  and using the matrix form of Eq. (5) we obtain  $dC^{(1)}/dz + (-\lambda + K^{(1)})C^{(1)} = 0$ , where  $K^{(1)} = R^T K R$ , and  $R^T = R^{-1}$  denotes the transpose of  $R$ . The reduced density matrix  $\rho_{nn'}^{(1)} = c_n^{(1)} c_{n'}^{(1)*}$  then satisfies the following equation:

$$\frac{d}{dz} \rho_{nn'}^{(1)} - \lambda_{nn'} \rho_{nn'}^{(1)} = - \sum_l [K_{nl}^{(1)} \rho_{ln'}^{(1)} + K_{n'l}^{(1)*} \rho_{nl}^{(1)}], \quad (6)$$

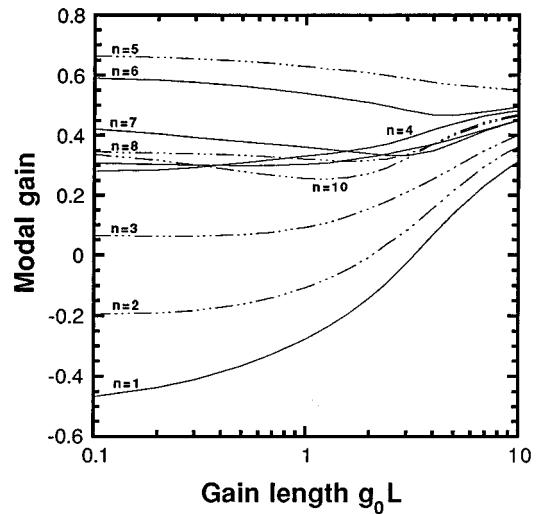


FIG. 2. Plot of modal eigenstate gain:  $\ln[\rho_{nn}^{(1)}(L)/\rho_{nn}^{(1)}(0)]/g_0 L$  for ten even-parity modes in a truncated parabolic medium,  $\hat{g}, \hat{h} = 1 - \tilde{x}^2$ ;  $|\tilde{x}| < 1$ , versus gain-length product  $g_0 L$  for  $F_e = 100$ ,  $\eta = 10$ ,  $\sigma_f = 0.1$ . The integer  $n = 1, \dots, 10$  labels the parabolic eigenstates in ascending order of  $\text{Re}(\lambda_n)$ .

where  $\chi_{nn'} = \chi_n + \chi_{n'}^*$ . We proceed to solve Eq. (6) by first solving for  $\rho_{nn'}^{(1)}$ , iterating the right-hand-side (rhs) and then taking ensemble averages. We first employ for  $\rho_{nn'}^{(1)}$  an envelope representation,  $\rho_{nn'}^{(1)} = \tilde{\rho}_{nn'} e^{\chi_{nn'} z}$ , and we assume the following decoupling [18] and an exponential form for the correlation function:

$$\begin{aligned} \langle K_{nl}^{(1)}(z) K_{n'l'}^{(1)}(z') \tilde{\rho}_{mk}(z') \rangle \\ \simeq \langle K_{nl}^{(1)}(z) K_{n'l'}^{(1)}(z') \rangle \langle \tilde{\rho}_{mk}(z') \rangle \\ = \langle K_{nl}^{(1)}(z) K_{n'l'}^{(1)}(z) \rangle e^{-q_f(z-z')} \langle \tilde{\rho}_{mk}(z') \rangle, \end{aligned} \quad (7)$$

which holds exactly for RTS [16]. Continuing as in Ref. [18], we next carry out the integration over  $z'$ , using  $\tilde{\rho}_{nn'}(z') \simeq \tilde{\rho}_{nn'}(z)$ , and then transform back from  $\rho_{nn'}$  to  $\rho_{nn'}^{(1)}$ . Upon redefining  $\rho_{nn'}^{(1)} \equiv \langle \rho_{nn'}^{(1)} \rangle$ , we finally obtain for the ensemble-averaged field equation

$$\begin{aligned} \frac{d}{dz} \rho_{nn'}^{(1)}(z) - \chi_{nn'} \rho_{nn'}^{(1)}(z) \\ = \sum_{l,l'} \left\{ \frac{\langle K_{nl}^{(1)} K_{l'l'}^{(1)} \rangle}{q_f + \chi_{l'} - \chi_l} \rho_{l'l'}^{(1)}(z) + \frac{\langle K_{n'l}^{(1)*} K_{l'l'}^{(1)*} \rangle}{q_f + \chi_{l'}^* - \chi_l^*} \rho_{n'l'}^{(1)}(z) \right. \\ \left. + \langle K_{n'l'}^{(1)*} K_{nl}^{(1)} \rangle \left[ \frac{1}{q_f + \chi_l - \chi_n} + \frac{1}{q_f + \chi_{l'}^* - \chi_n^*} \right] \rho_{l'l'}^{(1)}(z) \right\}. \end{aligned} \quad (8)$$

To choose a cutoff  $l_M$  for the number of eigenmodes (of both parities), we first include only modes that contribute significantly to the rhs of Eq. (8), i.e.,  $|\chi_n - \chi_{n'}| \ll q_f$ . A physical (and generally more restrictive) criterion follows from excluding those modes that refract out of the lasing plasma [7],  $\text{Im}(\chi_n) \leq F_e \eta / 2$ . For example, the truncated parabolic profile used below (for  $F_e = 100$ ,  $\eta = 10$ ) can be shown to require about 30 modes.

For square profile eigenstates, we easily find, using Eq. (3),

$$\langle K_{nl}^{(1)} K_{n'l'}^{(1)} \rangle = 4 \langle (dx_0/dz)^2 \rangle \left[ \frac{\alpha_n \alpha_l \alpha_{n'} \alpha_{l'}}{(\alpha_n^2 - \alpha_l^2)(\alpha_n^2 - \alpha_{l'}^2)} \right]. \quad (9)$$

Using Eq. (9) in Eq. (8) with the condition  $|\chi_n - \chi_{n'}| \ll q_f$ , reintroducing unnormalized units, and using  $q_f \simeq 1/l_s$ , we obtain a convenient parametrization for the strength of the fluctuation terms appearing on the rhs of Eq. (8):

$$\sigma_f = 4 l_s \langle (dx_0/dz)^2 \rangle / g_0 a^2 = 4 \langle x_0^2 \rangle q_f / g_0 a^2. \quad (10)$$

We now evaluate Eq. (8) for several values of  $\sigma_f$ , assuming equal occupation for each state  $\rho_{nn'}$  at small  $g_0 z$  and using  $\rho_{nn'}^{(1)} = \sum_{l,l'} R_{nl}^T \rho_{ll'} R_{l'n'}^*$ . We use the modal representation for the electric field correlation function,  $I_c(\tilde{x}_1, \tilde{x}_2; z) = \sum_{nn'} \rho_{nn'}(z) u_n(\tilde{x}_1) u_n^*(\tilde{x}_2)$ , and we define a transverse coherence length as the distance  $x_c$  over which the absolute value of the complex coherence factor  $\mu = |I_c(0, \tilde{x}) / \sqrt{I_c(0,0) I_c(\tilde{x}, \tilde{x})}|$  drops from unity at  $\tilde{x}_c = 0$  to  $\sin(1) \simeq 0.84$ . Truncated parabolic profiles for the gain and

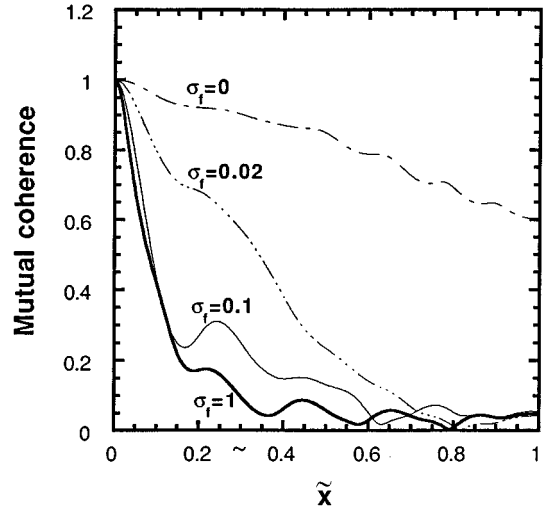


FIG. 3. Mutual coherence profiles for several values of the fluctuation strength parameter  $\sigma_f$  versus normalized transverse coordinate  $\tilde{x}$  for gain-length product  $g_0 L = 10$ ,  $F_e = 100$ ,  $\eta = 10$ , and  $l_M = 20$ . Gain  $\hat{g}$  and electron density profiles  $\hat{h}$  are as in Fig. 2.

electron density profiles are considered:  $\hat{g}, \hat{h} = 1 - \tilde{x}^2$ ,  $|\tilde{x}| < 1$ . In the following, we consider a spectrum of  $l_M = 20$  modes (10 even and 10 odd) as a satisfactory compromise between computational accessibility and a meaningful characterization of the role of fluctuations on coherence.

In Fig. 2 we display how the normalized modal “gain coefficients,” i.e.,  $\ln[\rho_{nn}^{(1)}(L)/\rho_{nn}^{(1)}(0)]/g_0 L$ , evolve with increasing gain length product: negative gain modes become positive gain modes while strongly growing modes undergo some reduction in amplification. These features clearly suggest how fluctuations may degrade coherence through reduced gain discrimination. In addition, the possibility for overall gain reduction exists for larger values of  $\sigma_f$ . This is particularly important for rounded transverse gain profiles

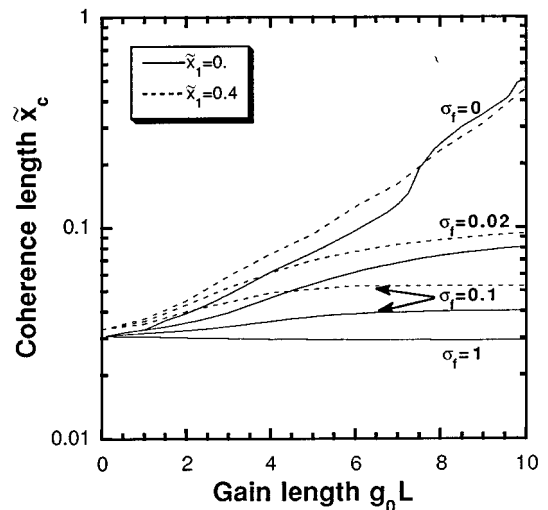


FIG. 4. Coherence length  $\tilde{x}_c$  versus gain-length product  $g_0 L$  for several values of fluctuation strength parameter  $\sigma_f$  and off-axis transverse coordinate  $\tilde{x}_1 = 0, 0.4$ . Parameters, spectrum and profiles are as in Fig. 3.

that have a fewer number of strongly growing modes compared to the case of a square profile (which we have also analyzed but not presented).

In Fig. 3 are shown coherence profiles  $\mu$  for several values of  $\sigma_f$ . We note how strongly the coherence is degraded for  $\sigma_f$  as small as 0.02 with coupling between only 20 modes. (For  $l_M=30$  and  $\sigma_f=0.1$ ,  $\tilde{x}_c$  is further reduced by 10%).

In Fig. 4 we plot the coherence length versus gain length product. Again, the trend towards limitation of coherence with increasing gain-length product is quite evident. Also from Fig. 4 we see that this feature persists for off-axis coherence ( $\tilde{x}_1 \neq 0$ ), which is more representative of Nova coherence experiments [2]. This insensitivity to  $x_1$  is expected because of the general  $\rho_{nn'}(z)$  dependence of transverse coherence, which saturates with increasing laser length. An insensitivity of transverse coherence length to laser length is seen in Nova coherence experiments [2], but the associated large values of  $F_e$  ( $\approx 4800$ ) and  $\eta$  ( $\approx 100$ ) render unwieldy a quantitative study due to the prohibitively large number of modes ( $l_M \approx 300$ ). However, a similar (and even stronger) effect is expected based on properties of the mode spectrum for large Fresnel number where a group of strongly bound states exchanges gain strength with a larger number of increasingly coupled [ $K_{nn}^{(1)} \approx n^2 \sigma_f$ , see Eq. (9)] set of weakly bound or low gain modes.

The parameter space considered in this paper, i.e.,  $F_e=100$ ,  $\eta=10$ , is associated with satisfactorily large coherence lengths for x-ray holography in the absence of fluctuations. Because  $\sigma_f$  is on the order of 0.1 in Nova experiments, substantial degradation of transverse coherence from fluctuations is expected.

An obvious means of testing the role of laser nonuniformities on saturated coherence in Nova two-beam x-ray laser experiments is to implement various amounts of beam smoothing. Random phase plates [5] and smoothing by spectral dispersion [19] are generally not effective in the near field of the laser; e.g., as *along* a line focus, and alternative smoothing techniques are needed. One technique is to superimpose several parts of the beam (as in a segmented wedge array [20], for example) to homogenize the line focus. Another approach is to use plasma buffering for smoothing of laser nonuniformities [21]. In these ways it may be possible to reduce  $\sigma_f$  to below 0.01 and achieve greatly improved transverse coherence.

Useful discussions with S. Dixit and R. Ehrlich are gratefully acknowledged. This work was performed under the auspices of the U.S. Department of Energy by the Lawrence Livermore National Laboratory under Contract No. W-7405-ENG-48.

- 
- [1] R. A. London, M. D. Rosen, and J. E. Trebes, *Appl. Opt.* **28**, 3397 (1989).
- [2] J. E. Trebes *et al.*, *Phys. Rev. Lett.* **68**, 588 (1992).
- [3] A. Carrillon *et al.*, *Phys. Rev. Lett.* **8**, 618 (1991); B. J. MacGowan *et al.*, *Phys. Fluids B* **4**, 2326 (1992).
- [4] J. G. Lunney, *Appl. Phys. Lett.* **48**, 891 (1986); R. Kodama *et al.*, *Phys. Rev. Lett.* **73**, 3215 (1994).
- [5] R. A. London, M. Strauss, and M. D. Rosen, *Phys. Rev. Lett.* **65**, 563 (1990).
- [6] P. Amendt, R. A. London, and M. Strauss, *Phys. Rev. A* **44**, 7478 (1991).
- [7] P. Amendt, R. A. London, and M. Strauss, *Phys. Rev. A* **47**, 4348 (1993).
- [8] M. D. Feit and J. A. Fleck, Jr., *J. Opt. Soc. Am. B* **7**, 2048 (1990).
- [9] G. Hazak and A. Bar-Shalom, *Phys. Rev. A* **40**, 7055 (1989).
- [10] R. A. London, *Phys. Fluids B* **5**, 2707 (1993).
- [11] G. Hazak and A. Bar-Shalom, *Phys. Rev. A* **38**, 1300 (1988).
- [12] Zahavi, G. Hazak, and Z. Zinamon, *J. Opt. Soc. Am. A* **9**, 1807 (1992); *J. Opt. Soc. Am. B* **10**, 271 (1993).
- [13] R. P. Ratowsky and R. A. London, *Phys. Rev. A* **51**, 2361 (1995).
- [14] S. N. Dixit *et al.*, *Inertial Confinement Fusion* **3**, 90 (1993).
- [15] G. Zimmerman and W. Kruer, *Comments Plasma Phys. Controlled Fusion* **2**, 85 (1975).
- [16] B. W. Shore, *J. Opt. Soc. Am. B* **1**, 176 (1984); K. Wodkiewicz, B. W. Shore, and J. H. Eberly, *ibid.* **1**, 398 (1984); J. H. Eberly, K. Wodkiewicz, and B. W. Shore, *Phys. Rev. A* **30**, 2381 (1984); K. Wodkiewicz, B. W. Shore, and J. H. Eberly, *ibid.* **30**, 2390 (1984); G. Hazak, M. Strauss, and J. Oreg, *ibid.* **33**, 3475 (1985).
- [17] Completeness has previously been argued when the free mode portion of the spectrum, i.e.,  $\lim_{|\tilde{x}| \rightarrow \infty} u_E(\tilde{x}) < \infty$  [7], is appended to the (*positive* gain) bound mode portion of the spectrum, i.e.,  $\lim_{|\tilde{x}| \rightarrow \infty} u(\tilde{x}) = 0$ . Recently, we have developed a simplified version of completeness that replaces the free mode continuum with discrete *negative* gain eigenmodes [Author (unpublished)].
- [18] M. Strauss, P. Amendt, H. U. Rahman, and N. Rostoker, *Phys. Rev. Lett.* **55**, 406 (1985); P. Amendt, M. Strauss, H. U. Rahman, and N. Rostoker, *Phys. Rev. A* **33**, 839 (1986).
- [19] S. Skupsky *et al.*, *J. Appl. Phys.* **66**, 3456 (1989); H. T. Powell, S. N. Dixit, and M. A. Henesian, *Inertial Confinement Fusion* **1**, 1 (1990).
- [20] D. M. Villeneuve, G. D. Enright, H. A. Baldis, and J. C. Kieffer, *Opt. Commun.* **81**, 54 (1991).
- [21] M. Desselberger *et al.*, *Phys. Rev. Lett.* **68**, 1539 (1992).